Monatsh Chem (2010) 141:859–865
DOI 10.1007/s00706-010-0336-y

ORIGINAL PAPER

Oxidation of ethylbenzene (derivatives) catalyzed by a functionalized ionic liquid combined with cationic (tetrakis(*N*-methyl-4-pyridinium)porphyrinato)manganese(III) and anionic phosphotungstate

Wei Liu · Qing-Xia Wan · Ye Liu

Received: 12 January 2010 / Accepted: 20 May 2010 / Published online: 18 June 2010

Abstract A functionalized ionic liquid (IL) combined with cationic (tetrakis(*N*-methyl-4-pyridinium)porphyrinato)manganese(III) and anionic phosphotungstate was prepared and applied as the catalyst for ethylbenzene (derivative) oxidations without involvement of the auxiliary axial ligands. A synergetic catalytic effect between the cations and the counteranions in this functionalized IL was observed in terms of activity and stability. Although anionic phosphotungstate ($[PW_{12}O_{40}]^{3-}$) showed negligible contribution to the activation of ethylbenzene, it stabilized the manganese porphyrin against oxidative degradation. The in situ UV-Vis analysis of the oxidation of the functionalized IL by PhIO indicated that with the incorporation of $[PW_{12}O_{40}]^{3-}$ as the counteranion the formation of the μ-oxo Mn^{IV} porphyrin dimer was completely suppressed, resulting in improved catalytic performance for the corresponding manganese porphyrin.

Keywords Functionalized ionic liquid · Manganese porphyrin · Metalloporphyrin · Polyoxometallate · Catalytic oxidation

Introduction

Ionic liquids (ILs) have been widely used as reaction media, which can offer better reaction selectivity, higher yields, and recyclability with 'green' attributes, although some of their properties, like good chemical stability, volatility, etc., have been challenged [1–5]. By varying the cations and anions that constitute the IL's structure, it is possible to design ILs with the required functionalities [6]. This strategy may provide ways to reinforce the catalytic behavior exerted by the cations and anions synergistically, which is regarded as particularly important not only for the design of liquid-phase catalysis experiments, but also for the development of hybrid organic/inorganic functional materials with diverse properties [7, 8].

Metalloporphyrins are well known for their ability to catalyze oxidation of hydrocarbons by using single oxygen atom donors, such as iodosylbenzene (PhIO), hypochlorites, and hydroperoxides [9, 10]. All metalloporphyrins suffer from deactivation, oxidative degradation, intermolecular self-aggregation through π–π interaction, and susceptibility to the formation of an unreactive μ-oxo porphyrin dimer ((por)M–O–M(por)) [10–12]. Many strategies have been developed to tune the reactivity of metalloporphyrins, including the introduction of bulky and/or electron-withdrawing substituents at *meso* positions, and the use of nitrogenous bases as axial ligands [13–15].

On the other hand, heteropolyanion salts (or polyoxometalates, POMs) have been widely investigated as 'green' catalysts in the oxidation of hydrocarbons [16–18]. The associations of heteropolyanions with organic groups, like benzotriazole [19], 2,2′-biquinoline [20], 8-hydroxyquinoline [21, 22], urea [23], and glycine [24], have been described with potential optical, magnetic, or electric properties rather than as catalysts. Associations of heteropolyanions with metal complexes like metalloporphyrins have been scarcely reported [25, 26].

In order to exploit the individual catalytic properties of metalloporphyrin and heteropolyanions, in this study, the ionic compound combined with cationic (tetrakis(*N*-

W. Liu · Q.-X. Wan · Y. Liu (✉)
Shanghai Key Laboratory of Green Chemistry and Chemical Processes, Chemistry Department,
East China Normal University,
3663 North Zhongshan Road, Shanghai, China
e-mail: yliu@chem.ecnu.edu.cn

methyl-4-pyridinium)porphyrinato)manganese(III) and anionic phosphotungstate (**2**, Scheme 1) was prepared and applied as a catalyst for ethylbenzene oxidation without additional involvement of the axial ligands. In regard to the matched compatibility (miscibility), the room temperature IL *N*-butylpyridinium tetrafluoroborate ([Bpy]BF_4) was used as the corresponding solvent. For comparison, (tetrakis(*N*-methyl-4-pyridinium)porphyrinato)manganese(III) hexafluorophosphate ($[Mn^{III}TMPyP][PF_6]_5$, **1**) [27] and *N*-butylpyridinium phosphotungstate ($[Bpy]_3[PW_{12}O_{40}]$, **3**) [28] were prepared and investigated in parallel.

Results and discussion

*Synthesis and characterization of **1** and **2***

Since (tetrakis(*N*-methyl-4-pyridinium)porphyrinato)manganese(III) iodide salt and α-Keggin-type phosphotungstic acid ($H_3[PMo_{12}O_{40}]\cdot xH_2O$) are highly soluble in water, the association of $[PMo_{12}O_{40}]^{3-}$ anions with large cations of $[Mn^{III}TMPyP]^{5+}$ leads to the precipitation of insoluble compounds. This behavior guaranteed the desired association of the cationic Mn porphyrins with $[PW_{12}O_{40}]^{3-}$ anions at the stoichiometric ratio.

Thermogravimetry/differential thermal gravimetry (TG/DTG) analyses (Fig. 1) indicated that the thermal stabilization of **2** was dramatically improved in comparison to that of **1**, and that the $[PW_{12}O_{40}]^{3-}$ anion (in **2** and **3**) was thermally stable up to 800 °C. Compound **1** was destructed at ca. 310 °C due to the dissociation of unstable PF_6^- anions. Compound **2** decomposed at ca. 520 °C, corresponding to the collapse of the porphyrin framework. TG/DTG analysis also revealed that the stoichiometric ratio of $[Mn^{III}TMPyP]^{5+}$ to $[PW_{12}O_{40}]^{3-}$ in **2** was 0.6, which was consistent with 13.5% weight loss over the range 400–750 °C due to the CHN loss for the porphyrin ring system. The stoichiometric ratio of $[Bpy]^+$ to $[PW_{12}O_{40}]^{3-}$ in **3** was determined to be 3, according to 12.6% weight loss over the range 350–600 °C.

FT-IR spectra in Fig. 2 showed that for **2** the characteristic bands of the typical α-Keggin-type $[PW_{12}O_{40}]^{3-}$ were observed in the region of 1,100–600 cm^{-1} without significant changes in comparison to those of $H_3[PW_{12}O_{40}]$ (1,077 ($P–O_a$), 978 (terminal $W–O_d$), 896 (inter-octahedral $W–O_b–W$), 800 (intra-octahedral $W–O_c–W$) cm^{-1}) [29]. Besides these bands, the peaks at 3,100–3,000 cm^{-1} ascribed to C–H vibrations, and 1,638 cm^{-1} ascribed to C=N vibration in the porphyrin ring were observed, implying the desired association of the cationic $[Mn^{III}TMPyP]^{5+}$ with $[PW_{12}O_{40}]^{3-}$ anions. The UV-Vis spectra of **2** in DMF (Fig. 2) showed the typical absorbance bands corresponding to the cationic $[Mn^{III}TMPyP]^{5+}$ (Soret band, 462 nm; Q bands, 564 and 600 nm) and $[PW_{12}O_{40}]^{3-}$ (CT band, 268 nm), respectively. The spectroscopic characterization of **2** by FT-IR and UV-Vis indicated that the individual properties of the cations and the anions in **2** were not altered dramatically, suggesting a simple charge interaction between them [26].

*The catalytic performance of **2** in ethylbenzene oxidation*

The oxidation of ethylbenzene was selected as a model reaction to evaluate the catalytic performance of **2**. The reaction conditions were optimized in terms of solvents ([Bpy]BF_4 and DMF), oxidants (PhIO, H_2O_2, $PhI(OAc)_2$, NaClO, and *m*-chloroperoxybenzoic acid), catalyst concentration, molar ratio of oxidant to substrate, reaction time, and temperature. Under the optimal conditions (0.4 mol% catalyst, [Bpy]BF_4 as a solvent, 1.5 equiv. of PhIO, 1 h, 30 °C), **2** exhibited better activities than **1** (entry 2 vs. 1, Table 1), suggesting that the incorporation of $[PW_{12}O_{40}]^{3-}$ gave rise to the activation of ethylbenzene. The formation of ketone was due to the further oxidation of alcohol by excess PhIO. In order to further explain the role of the $[PW_{12}O_{40}]^{3-}$ anion in ethylbenzene oxidation, the

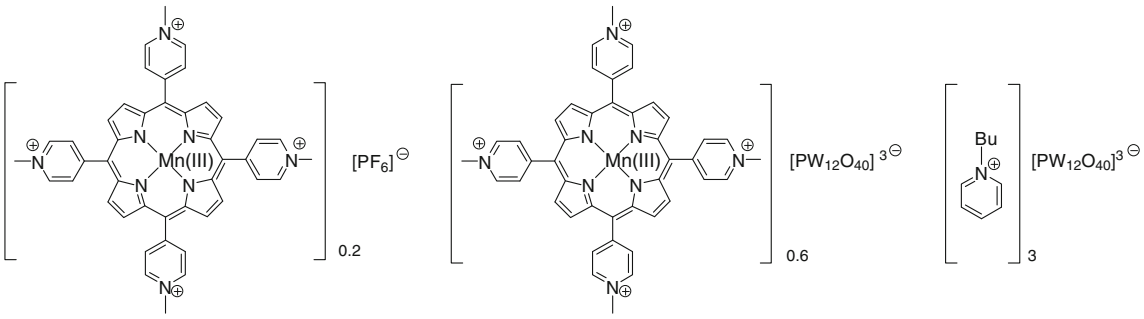

$[Mn^{III}TMPyP][PF_6]_5$ (**1**) $[Mn^{III}TMPyP]_{0.6}[PW_{12}O_{40}]$ (**2**) $[Bpy]_3[PW_{12}O_{40}]$ (**3**)

Scheme 1

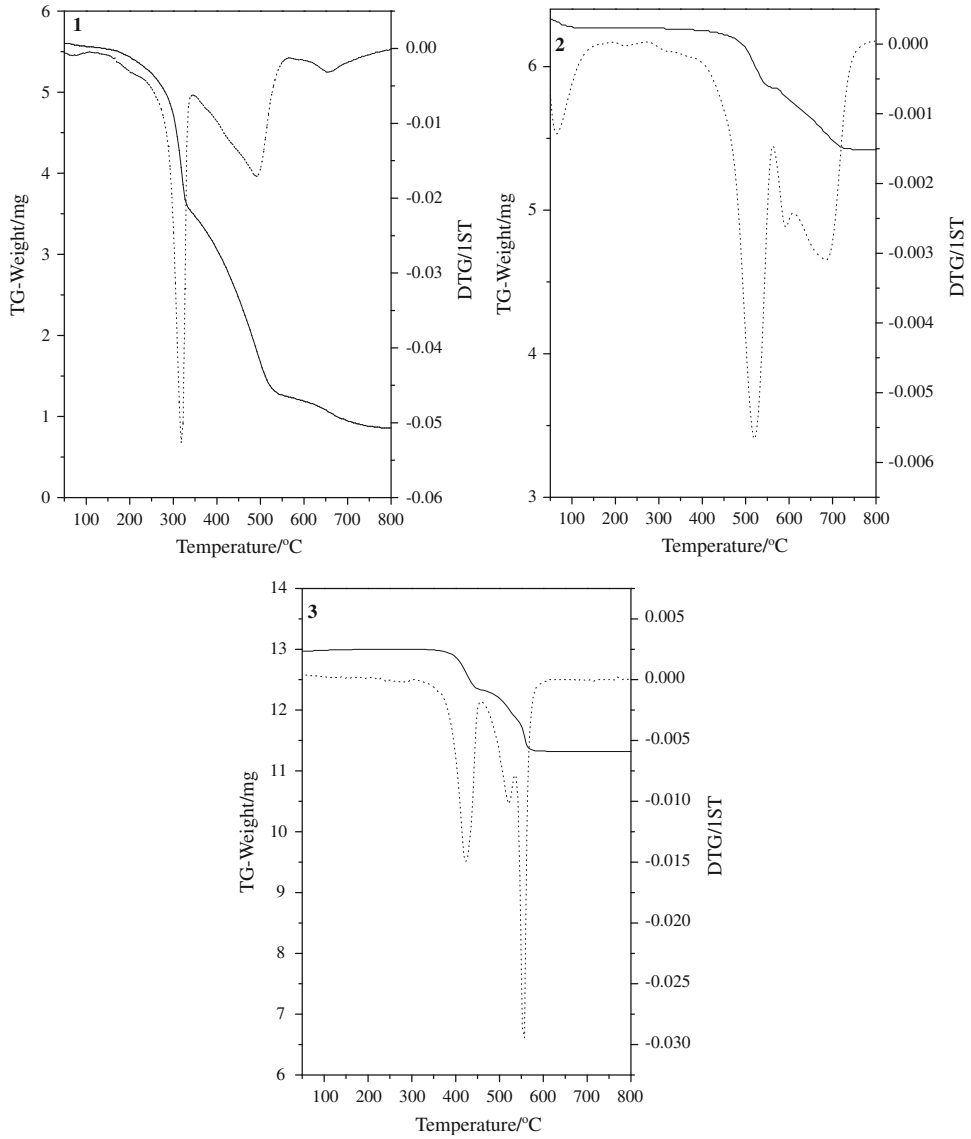

Fig. 1 TG/DTG analyses of **1–3** in air flow

activity of **3** in [Bpy]BF_4 was examined in entry 3, which indicated that the contribution of $[PW_{12}O_{40}]^{3-}$ to the activation of ethylbenzene was negligible.

Repeated use of **2** in [Bpy]BF_4 (Table 2) showed that **2** could be recycled for 4 runs without much activity loss. The UV-Vis spectra showed that after 4 runs, the typical Soret band of **2** (470 nm) was still clearly observed. In the absence of $[PW_{12}O_{40}]^{3-}$, the activity of **1** was lost rapidly with accompanying rapid decay of its Soret band. These results implied that the stability of **2** against oxidative degradation was greatly improved in comparison to that of **1**.

*In situ oxidation of **1** and **2** by PhIO monitored by UV-Vis spectroscopy*

The results in Table 1 showed that $[PW_{12}O_{40}]^{3-}$ exhibited no contribution to the activation of ethylbenzene. However, the improved catalytic behavior of **2** in terms of activity and stability was observed undoubtedly. In order to elucidate the specific role of $[PW_{12}O_{40}]^{3-}$ in **2**, the evolving oxidation of **2** by PhIO was monitored by UV-Vis spectroscopy.

The oxidation of **1** and **2** in [Bpy]BF_4 by PhIO was analyzed at ambient temperature. Because the behavior of the Mn porphyrin units was considered solely, the spectra in the region 380–650 nm was recorded. The UV-Vis spectra (Fig. 3a) showed that the typical Soret band (470 nm) and Q bands (574 and 610 nm) of **1** were observed in the first 30 min, but were accompanied by a slight decay due to the oxidative degradation. After ca. 30 min, a new peak at ca. 430 nm, which was assigned to the μ-oxo Mn^{IV} porphyrin dimer [10–12], gradually grew to reach a maximum intensity accompanied by the concurrent decay of absorbance at 470 nm. Once the μ-oxo

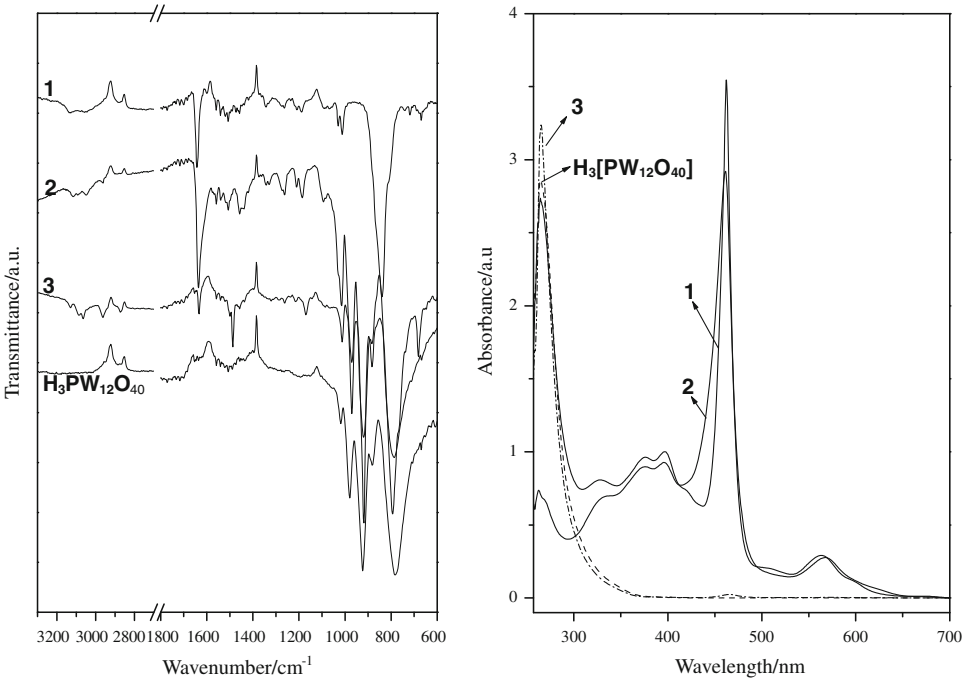

Fig. 2 FT-IR (KBr) and UV-Vis (DMF) spectra of **1–3**

Table 1 Comparison of catalysts **1–3** for ethylbenzene oxidation

Entry	Catalyst	Solvent	Conversion (%)	Selectivity (%)	
				1-Phenylethanol	1-Phenylethanone
1	**1**	$[Bpy]BF_4$	39	71	29
2	**2**	$[Bpy]BF_4$	53	56	44
3	**3**	$[Bpy]BF_4$	<3	–	–
4	**1**	DMF	17	10	90
5	**2**	DMF	23	8	92
6	**3**	DMF	<3	–	–

Catalyst 0.4 mol% (2 μmol), ethylbenzene 500 μmol, PhIO 750 μmol, solvent 2 cm^3, reaction temperature 30 °C, reaction time 1 h

Mn^{IV} porphyrin dimer was formed, it underwent more severe oxidative destruction than the corresponding Mn^{III} porphyrin complex due to the increased electron density in the porphyrin ring, which led to the large drop of the absorbance intensities for lines 6–9.

In contrast, when the oxidation of **2** by PhIO was monitored under the same conditions, the obtained UV-Vis spectra in Fig. 3b always exhibited the typical Soret band of **2** at ca. 470 nm without shifting during 60 min, revealing that the presence of the $[PW_{12}O_{40}]^{3-}$ counteranion in **2** as a π-electron-rich reservoir could suppress the formation of the less reactive μ-oxo Mn^{IV} porphyrin dimer, which could account for the improved activity and stability of **2** in $[Bpy]BF_4$ toward ethylbenzene oxidation. Hence, it was believed that the π–π interaction and the electrostatic force between $[Mn^{III}TMPyP]^{5+}$ cations and $[PW_{12}O_{40}]^{3-}$ anions in **2** could counteract the π–π stacking of porphyrin itself.

Comparatively, with DMF as the solvent, the oxidation of **2** or **1** by PhIO exhibited very similar spectral patterns like in Fig. 3c. In ca. 30 min, not only was the μ-oxo Mn^{IV} porphyrin dimer (435 nm) formed rapidly, but also the severe degradation of the manganese porphyrins occurred simultaneously. During 30 min monitoring, most of the Mn(III, IV) porphyrin complexes had been oxidatively destructed into non-conjugated fragments (line 6).

*Generality of **2**-[Bpy]BF_4 for oxidation of ethylbenzene derivatives*

To examine the generality of **2**-$[Bpy]BF_4$ catalysis, several ethylbenzene derivatives were selected and investigated and results are shown in Table 3. For the substrates without conjugated character, like *n*-hexane,

Table 2 Recycling of **1** and **2** in $[Bpy]BF_4$ for ethylbenzene oxidation

Run	**1**			**2**		
	Conversion (%)	Selectivity (%)		Conversion (%)	Selectivity (%)	
		X-ol[a]	X-one[a]		X-ol[a]	X-one[a]
1	39	71	29	53	56	44
2	30	30	70	50	30	70
3	24	26	74	51	27	73
4	15	25	75	51	27	73

Catalyst 0.4 mol%, ethylbenzene 500 μmol, PhIO 500 μmol, $[Bpy]BF_4$ 2 cm^3, reaction temperature 30 °C, reaction time 1 h

[a] X = 1-phenylethan

n-octane, *n*-chlorobutane, etc., the conversion was not detectable mainly due to the immiscibility of the substrate in the **2**-$[Bpy]BF_4$ system and the resultant mass transfer limitation. As shown in Table 3, with substituents possessing electron-donating nature (Me, OMe) at the *para* position of ethylbenzene, the increased electron density at the α carbon of ethylbenzene led to the fast formation of alkyl radicals and then the fast formation of the corresponding products (entries 1, 2). With electron-withdrawing groups (–Cl, –Br, –COOH) at *para* position, the conversions of the substrates were relatively low due to the decreased nucleophilicity at α carbon of the ethyl side chain (entries 3–5).

Conclusion

Without involvement of the auxiliary axial ligands, the ionic compound **2** combined with the cationic Mn porphyrin ($[Mn^{III}TMPyP]^{5+}$) and the α-Keggin-type phosphotungstate ($[PW_{12}O_{40}]^{3-}$) is an efficient catalyst in the room temperature IL $[Bpy]BF_4$ toward ethylbenzene oxidation in terms of activity and stability, in comparison to **1** which only possesses the catalytic site of $[Mn^{III}TMPyP]^{5+}$ alone. The contribution of $[PW_{12}O_{40}]^{3-}$ anions to the activation of ethylbenzene proved to be negligible, but to the stability of $[Mn^{III}TMPyP]^{5+}$ against the oxidative degradation was of significance. The in situ UV-Vis analysis for the oxidation of **2** by PhIO indicated that with the incorporation of $[PW_{12}O_{40}]^{3-}$ as the counteranions in **2** the formation of the μ-oxo Mn^{IV} porphyrin dimer with disadvantages of low reactivity and susceptibility to oxidative degradation was completely suppressed, which greatly favored the catalytic behavior of the corresponding $[Mn^{III}TMPyP]^{5+}$. In a general study only ethylbenzene derivatives with (partial) miscibility with $[Bpy]BF_4$ could be investigated. The substrates with electron-donating substituents (Me, OMe) at the *para* position of ethylbenzene afforded better conversions due to the increased electron density at the α carbon of ethylbenzene.

Experimental

Reagents and analyses

All chemical reagents were purchased and used as received. FT-IR spectra were recorded on a Nicolet NEXUS 670 spectrometer. The ^{31}P NMR spectra (with 85% H_3PO_4 sealed in a capillary tube as internal standard) were recorded on a Bruker Avance 500 spectrometer. The elemental analyses for Mn, P, and W were performed by an inductively coupled plasma (ICP) emission spectrometer (RIS Intrepid II XSP spectrometer, Thermo Electron Corporation). TG/DTG was acquired by using a Mettler TGA/SDTA 851^e instrument and STARe thermal analysis data processing system. TG/DTG measurements were run in air flow with a temperature ramp of 10 °C min^{-1} between 50 and 800 °C. GC analyses were performed on a SHIMADZU-14B chromatograph equipped with Rtx-Wax capillary column (30 m × 0.25 mm × 0.25 μm). GC–MS analyses were performed on an Agilent 6890 instrument equipped with Agilent 5973 mass-selective detector. UV-Vis spectra were recorded on a SHIMADZU-UV 2550 spectrophotometer with resolution of ca. 1 nm. The oxidation of **2** (or **1**) by PhIO in $[Bpy]BF_4$ or DMF was monitored in situ by means of their UV-Vis spectra. The mixture upon adding the catalyst (**1** or **2**), $[Bpy]BF_4$ (2 cm^3), and PhIO (20 mg, in large excess) into a UV cuvette (3 cm^3) was stirred until the appointed time.

Synthesis

Tetrakis(*N*-methyl-4-pyridinium)porphyrin iodide ($[H_2TMPyP][I]_4$) and (tetrakis(*N*-methyl-4-pyridinium)-porphyrinato)manganese(III) hexafluorophosphate (**1**) were prepared according to Ref. [27].

(Tetrakis(N-methyl-4-pyridinium)porphyrinato)-manganese(III) phosphotungstate ($[Mn^{III}TMPyP]_{0.6}[PW_{12}O_{40}]$) (**2**, $[C_{44}H_{36}N_8Mn]_{0.6}PW_{12}O_{40}$) (Tetrakis(*N*-methyl-4-pyridinium)porphyrinato)manganese (III) iodide [27] (207 mg) dissolved in 100 cm^3 deionized water was treated dropwise with 30 cm^3 of an aqueous solution of 1.0 g phosphotungstic acid $H_3[PW_{12}O_{40}]\cdot xH_2O$. A brown solid immediately precipitated from the solution. The resultant mixture was stirred vigorously at room temperature for 3 h. The brown precipitates were collected after centrifugation and then washed with deionized water and ethanol. A dark-brown product of **2** (352 mg) was

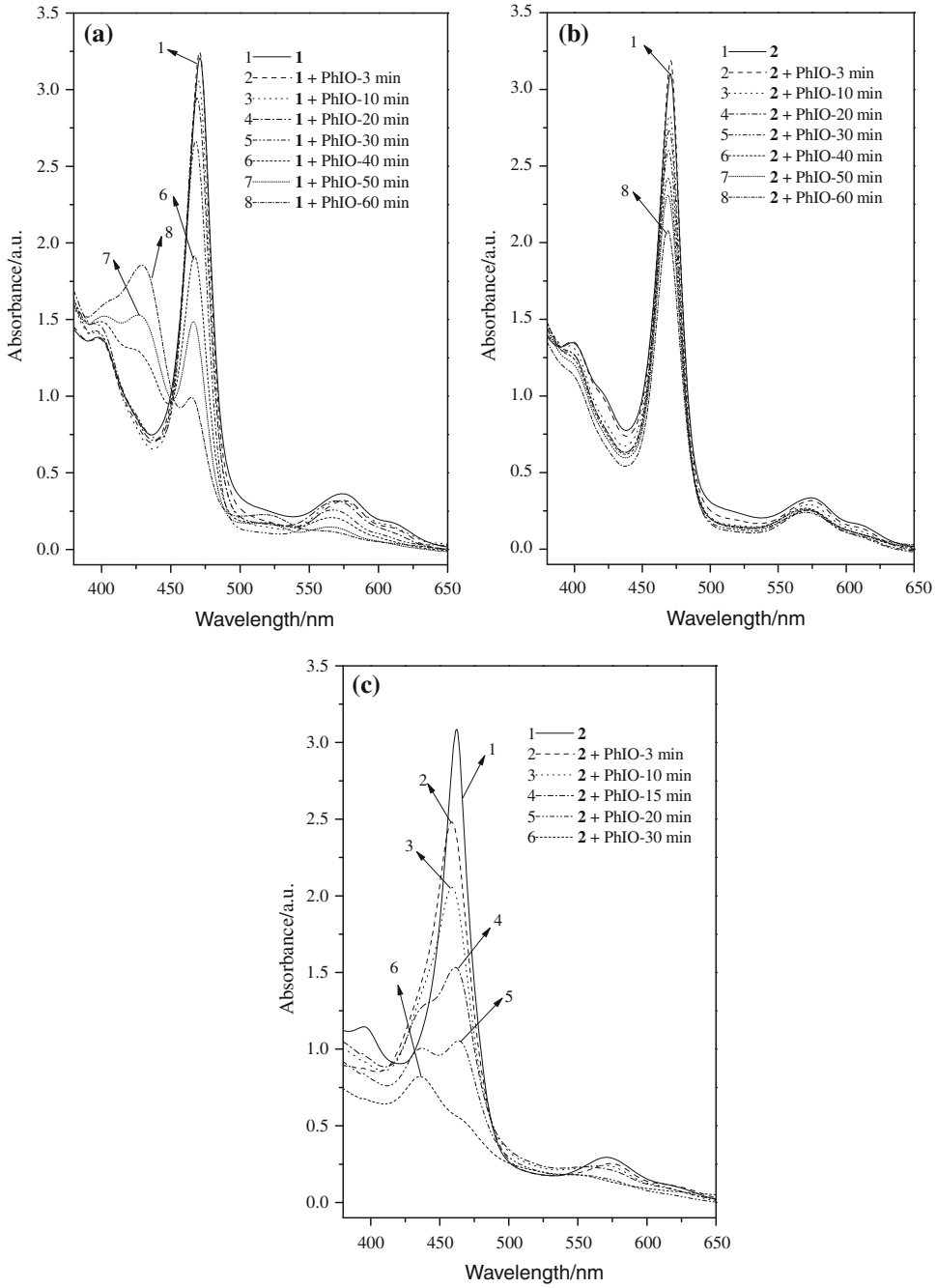

Fig. 3 UV-Vis spectra recorded for the continuously evolving processes of **a 1** oxidized by PhIO in $[Bpy]BF_4$; **b 2** oxidized by PhIO in $[Bpy]BF_4$; **c 2** oxidized by PhIO in DMF [conditions: **1** (or **2**) ca. 3.0×10^{-5} M, solvent 2 cm^3, PhIO 20 mg (in large excess), room temperature]

obtained after drying in vacuo. Due to the paramagnetism of **2**, its ^1H NMR signals were unobservable. UV-Vis (DMF): $\lambda_{max} = 268$ (s, CT transition of $[PW_{12}O_{40}]^{3-}$), 462 (s, Soret band), 564 and 600 (w, Q bands) nm; FT-IR (KBr): $\bar{\nu} = 3{,}099$ and 3,052 (w, C–H), 1,635 (m, C=N), 1,077 (P–O_a), 978 (terminal W–O_d), 896 (inter-octahedral W–O_b–W), 800 (intra-octahedral W–O_c–W) cm^{-1}.

N-Butylpyridinium phosphotungstate ($[Bpy]_3[PW_{12}O_{40}]$) (**3**) [28]

Compound **3** was prepared as described in Ref. [28] and then dried in an oven at 90 °C. ^{31}P NMR (200 MHz, DMF-d_6): $\delta = -14.0$ ppm; UV-Vis (DMF): $\lambda_{max} = 263$ nm; UV-Vis ($[Bpy]BF_4$): $\lambda_{max} = 304$ nm; FT-IR (KBr): $\bar{\nu} = 3{,}136$ (w), 3,080(w), 2,965(w), 2,936(w), 2,871(w), 1,633 (s, C=N), 1,483 (s, C=C), 1,083 (m, P–O_a), 982 (s, terminal W–O_d), 896 (m, inter-octahedral W–O_b–W), 808 (s, intra-octahedral W–O_c–W) cm^{-1}.

*General procedure for oxidation of ethylbenzene (derivatives) catalyzed by **2** in $[Bpy]BF_4$*

To 2 cm^3 $[Bpy]BF_4$ and 500 μmol ethylbenzene (analytical grade reagent used as received) was added 7 mg

Table 3 Oxidation of ethylbenzene derivatives catalyzed by **2** in $[Bpy]BF_4$

Entry	Substrate	Conversion (%)	Selectivity (%)[a]	
			Alcohol	Ketone
1	*p*-Methylethylbenzene	59	73	27
2	*p*-Methoxyethylbenzene	67	79	21
3	*p*-Chloroethylbenzene	51	53	47
4	*p*-Bromoethylbenzene	44	51	49
5	*p*-Carboxyethylbenzene	49	66	34

2 0.4 mol% (2 μmol), substrate 500 μmol, PhIO 750 μmol, $[Bpy]BF_4$ 2 cm^3, reaction temperature 30 °C, reaction time 1 h

[a] The product was identified further by GC–MS

catalyst **2** (2 μmol), yielding a totally homogeneous red-brown solution to which PhIO was then added to initiate oxidation at 30 °C. Upon completion, diethyl ether was added to extract the organic compounds (3×2 cm^3). The conversions of substrates were based on GC analyses with *n*-dodecane as internal standard. The selectivities of products were based on GC analyses with the normalization method. The products were further identified by GC–MS analysis.

The remaining ionic liquid phase was dried in vacuo and used without further treatment for next the run. In each run, due to the stoichiometric consumption of the oxidant, 110 mg PhIO (500 μmol) was added additionally besides the substrate.

Acknowledgments The research was financially supported by the National Natural Science Foundation of China (No. 20533010, 20673039), and the Science and Technology Commission of Shanghai Municipality (09JC1404800).

References

1. Smiglak M, Metlen A, Rogers RD (2007) Acc Chem Res 40:1182
2. Chowdhury S, Mohan RS, Scott JL (2007) Tetrahedron 63:2363
3. Swatloski RP, Holbrey JD, Rogers RD (2003) Green Chem 5:361
4. Earle MJ, Esperanca JMSS, Gilea MA, Lopes JNC, Rebelo LPN, Magee JW, Seddon KR, Widegren JA (2006) Nature 439:831
5. Wilkes JS (2004) J Mol Catal A Chem 214:11
6. Šebesta R, Kmentová I, Toma Š (2008) Green Chem 10:484
7. Lodge TP (2008) Science 321:50
8. Leng Y, Wang J, Zhu D, Ren X, Ge H, Shen L (2009) Angew Chem Int Ed 48:168
9. Kadish KM, Smith KM, Guilard R (eds) (2000) The porphyrin handbook, vol 3–4. Academic, San Diego, p 1
10. Iamamoto Y, Idemori YM, Nakagaki S (1995) J Mol Catal A Chem 99:187
11. Machado AM, Mypych F, Drechsel SM, Nakagaki S (2002) J Colloid Interface Sci 254:158
12. Groves JT, Lee J, Marla SS (1997) J Am Soc Chem 119:6269
13. Sheldon RA (ed) (1994) Metalloporphyrins in catalytic oxidations. Marcel Dekker, New York, p 1
14. Collman JP, Chien AS, Eberspacher TA, Zhong M, Brauman JI (2000) Inorg Chem 39:4625
15. Mohajer D, Sadeghian L (2007) J Mol Catal A Chem 272:191
16. Mizuno N, Yamaguchi K, Kamata K (2005) Coord Chem Rev 249:1944
17. Katsoulis DE (1998) Chem Rev 98:359
18. Neumann R (1998) Prog Inorg Chem 47:317
19. Han Z, Luang G, Wang E (2003) Trans Metal Chem 28:63
20. Gamelas JAF, Cavaleiro AMV, de Gomes EM, Belsley M, Herdtweck E (2002) Polyhedron 21:2537
21. Attanasio D, Bonamico M, Fares V, Imperatori P, Suber L (1990) J Chem Soc Dalton Trans 3221
22. Zhou Y, Wang E, Peng J, Liu J, Hu C, Huang R, You X (1999) Polyhedron 18:1419
23. Han Z, Wang E, You W, Liu S, Hu C, Xing Y, Jia H, Lin Y (2001) J Mol Struct 595:7
24. Bi L, He Q, Jia Q, Wang E (2001) J Mol Struct 597:83
25. Liu S, Xu J, Sun H, Li D (2000) Inorg Chim Acta 306:87
26. Santos ICMS, Rebelo SLH, Balula MSS, Martins RRL, Pereira MMMS, Simões MMQ, Neves MGPMS, Cavaleiro JAS, Cavaleiro AMV (2005) J Mol Catal A Chem 231:35
27. Liu Y, Zhang H, Lu Y, Cai Y, Liu X (2007) Green Chem 9:1114
28. Wang S, Liu W, Wan Q, Liu Y (1009) Green Chem 11:1589
29. Weng Z, Wang J, Jian X (2008) Catal Commun 9:1688